Open Access

Earth System
Science
Data

*Supplement of*

# Global ocean surface heat fluxes derived from the maximum entropy production framework accounting for ocean heat storage and Bowen ratio adjustments

**Yong Yang et al.**

*Correspondence to:* Huaiwei Sun (hsun@hust.edu.cn) and Wenxin Zhang (wenxin.zhang@glasgow.ac.uk)

# Fig. S1
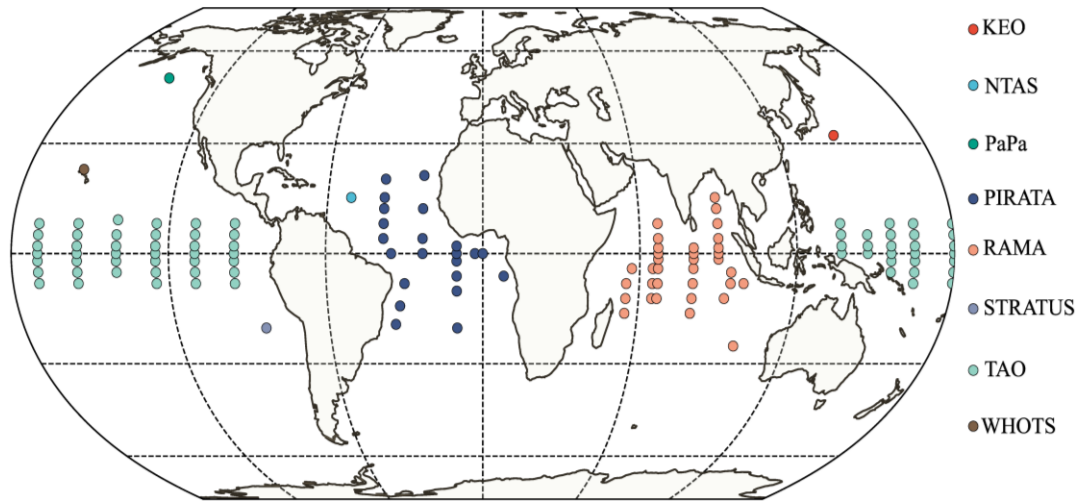


**Figure S1.** Spatial distribution map of buoy array sites used in this study

# Fig. S2
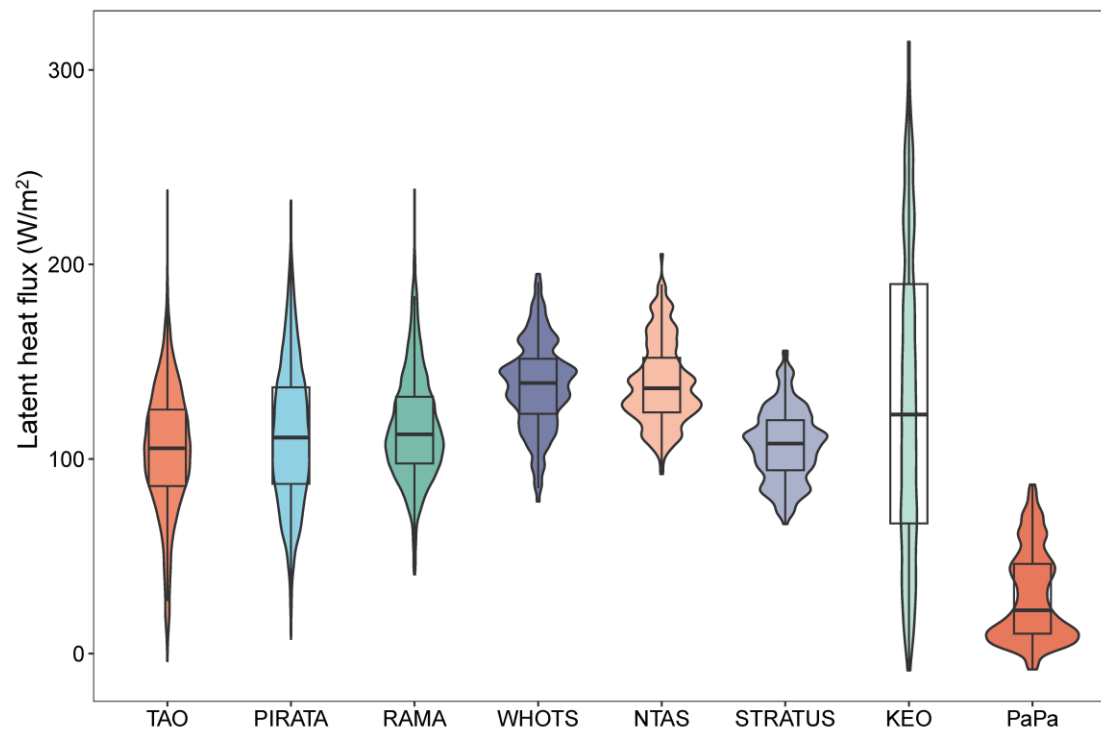


**Figure S2.** Violin plot of observations from distinct buoy arrays.

# Fig. S3
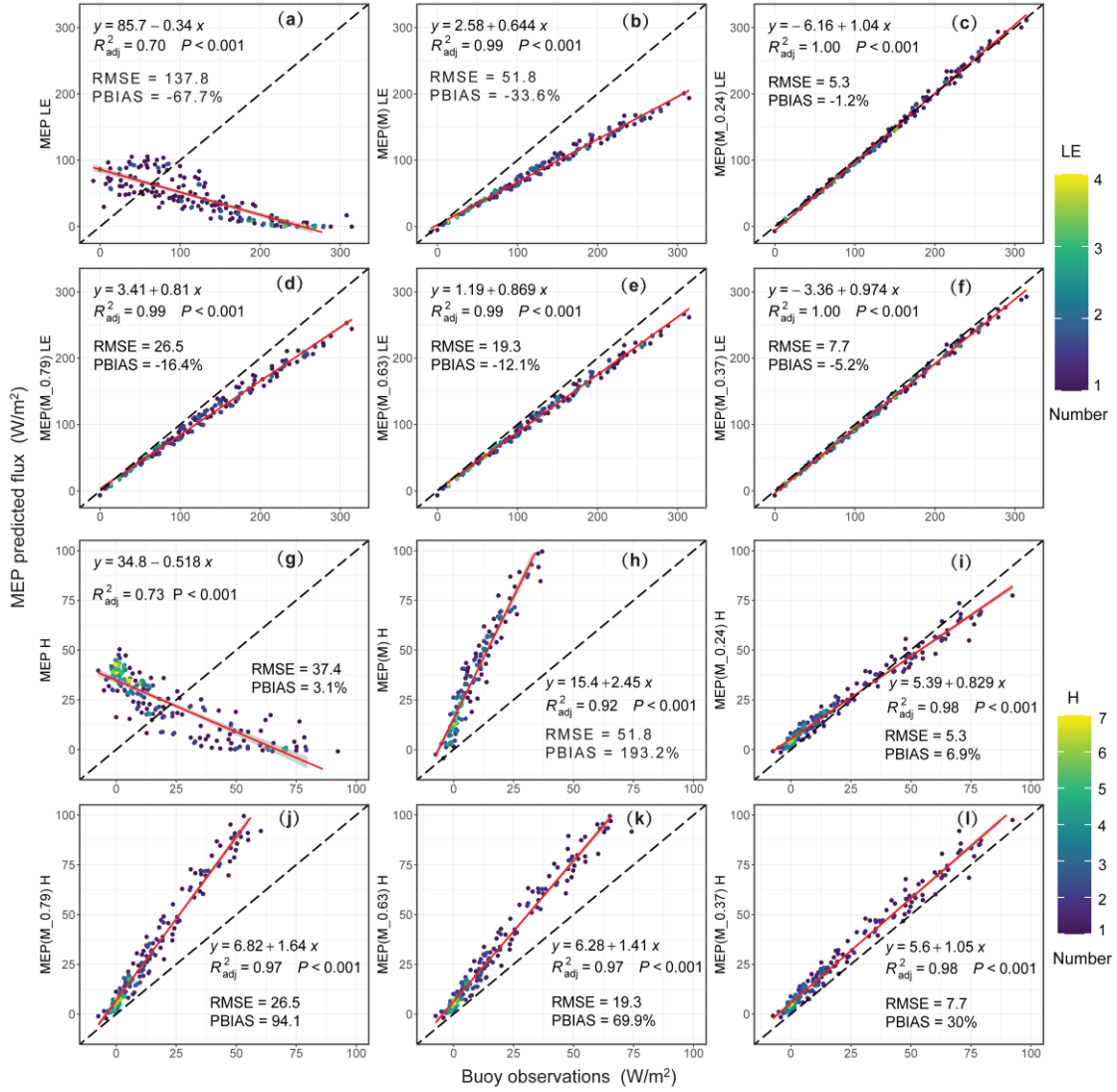


**Figure S3.** Scatter density plots of monthly latent heat flux (a~f) and sensible heat flux (g~l) derived by the original method and modified MEP method versus observations from the KEO buoy station for the period from June 17, 2004, to August 12, 2023. (a) The original MEP method, (b) The modified MEP method considering the heat storage effect, (c) The modified MEP method considering both the heat storage and empirical Bowen ratio formula $B_{oa}=0.24B_o{}^*$, (d)~(f) for the modified MEP method considering both the heat storage and empirical Bowen ratio formulas $B_{oa}=0.79B_o{}^*-0.21$, $B_{oa}=0.63B_o{}^*-0.15$, and $B_{oa}=0.37B_o{}^*-0.05$. (g)~(l) are the same with (a)~(f) but for sensible heat flux.

# Fig. S4
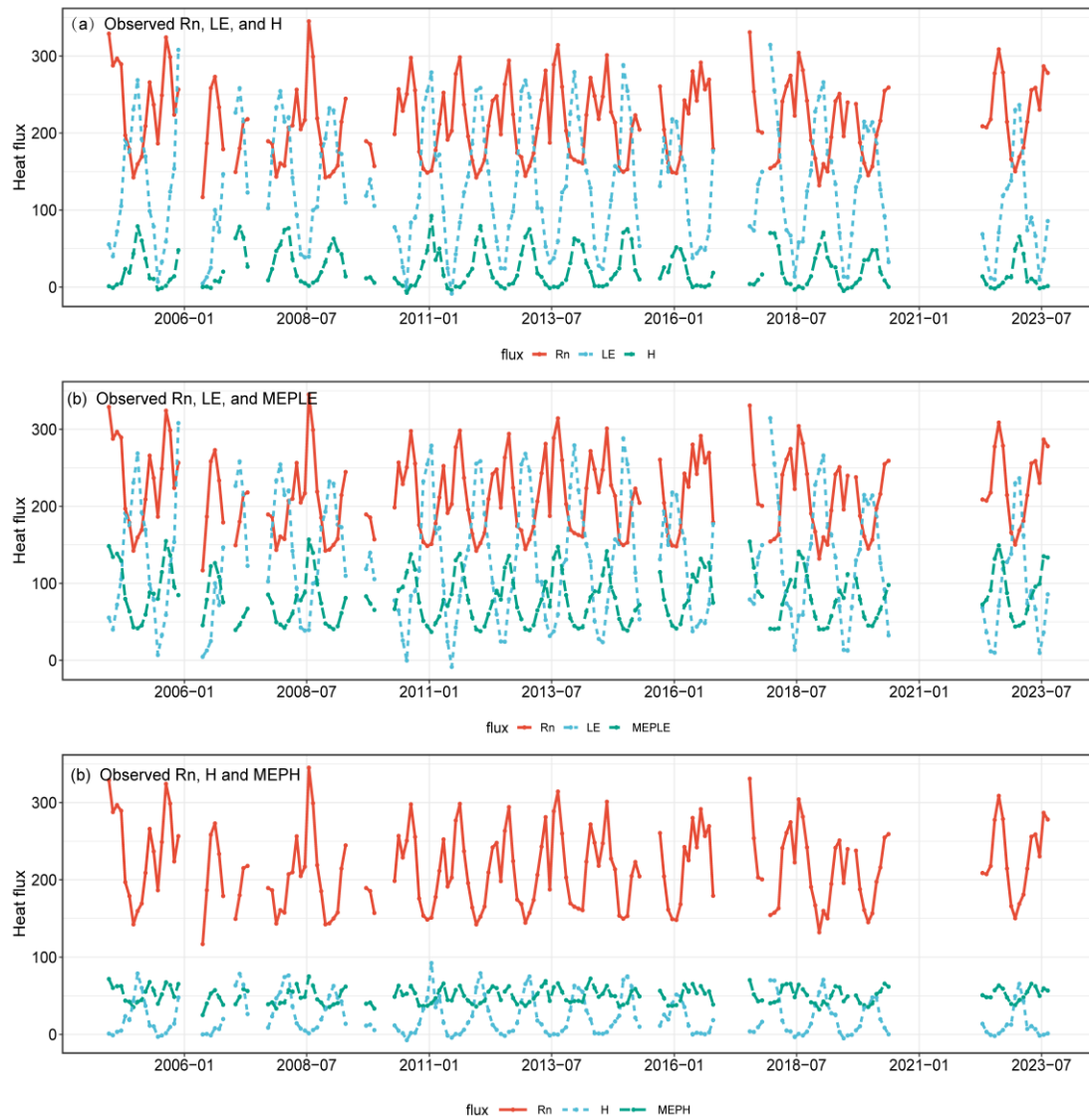


**Figure S4.** Comparisons of time series between MEP estimates and buoy observations. (a) Variations of observed net radiation ($R_n$), latent heat flux ($LE$), and sensible heat flux ($H$). (b) Variations of observed $R_n$, observed $LE$, and MEP estimated $LE$. (c) Variations of observed $R_n$, observed $H$, and MEP estimated $H$.

**Fig. S5**
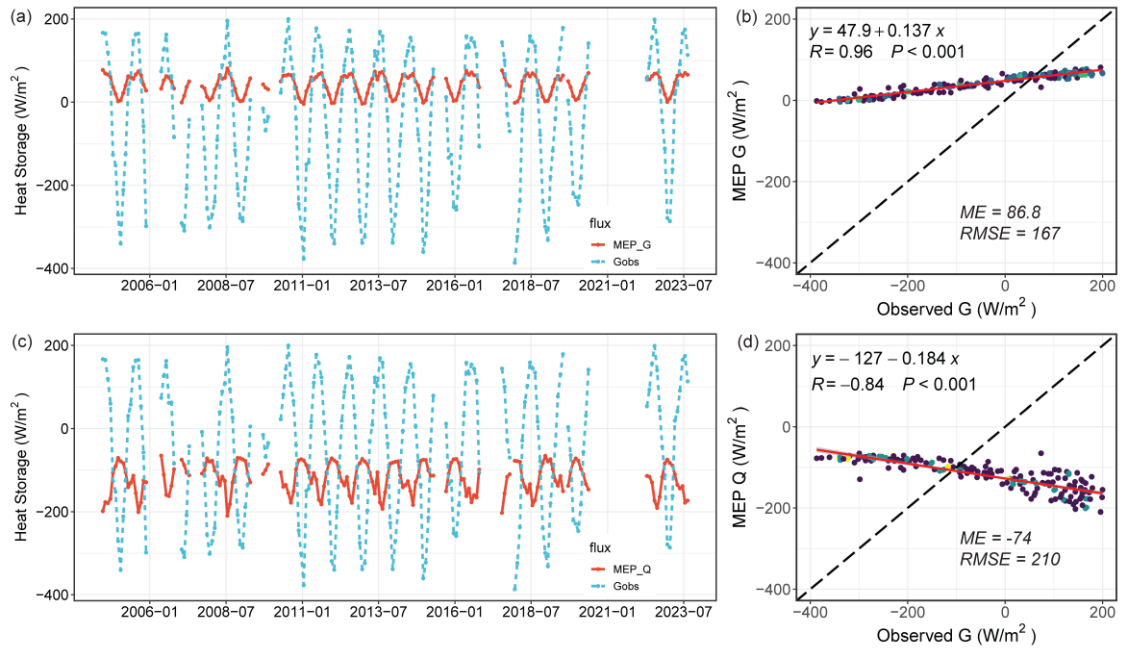


**Figure S5.** Comparisons of observed heat storage with predicted heat storage (a) and surface thermal energy flux $Q$ (c) by the original MEP method, along with corresponding scatter plots (b, d) at KEO sites. *Gobs* represents observed heat storage, *MEP_Q* denotes surface thermal energy flux, and *MEP_G* represents heat storage predicted by the original MEP method.

# Fig. S6
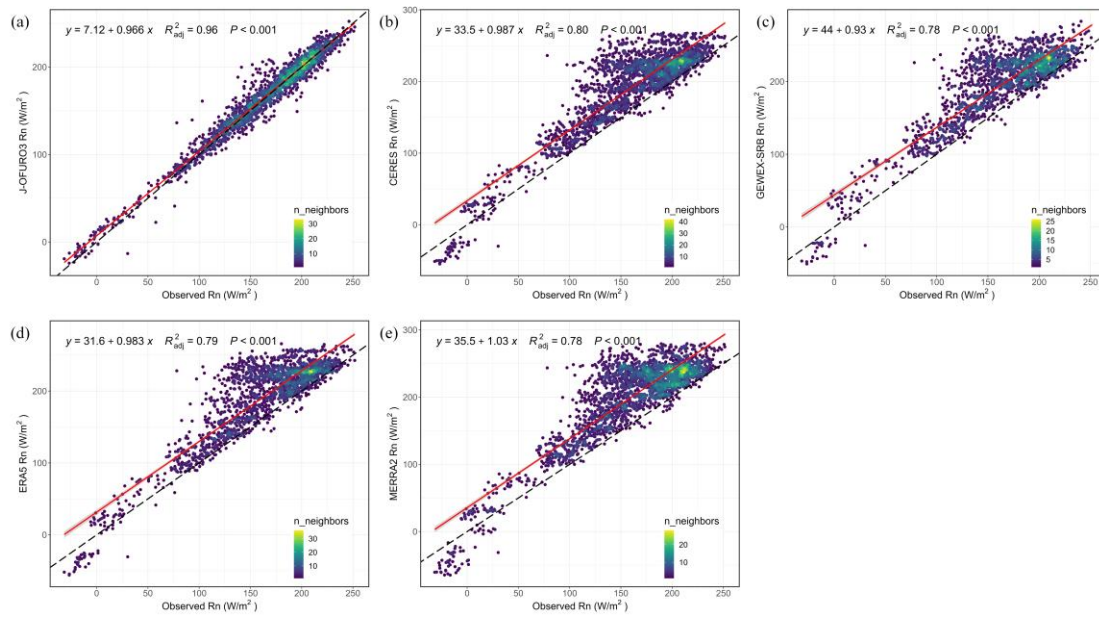


**Figure S6.** Assessment of net radiation derived from different datasets against buoy observations: (a) J-OFURO3, (b) CERES, (c) GEWEX-SRB, (d) ERA5, and (e) MERRA2.

# Fig. S7
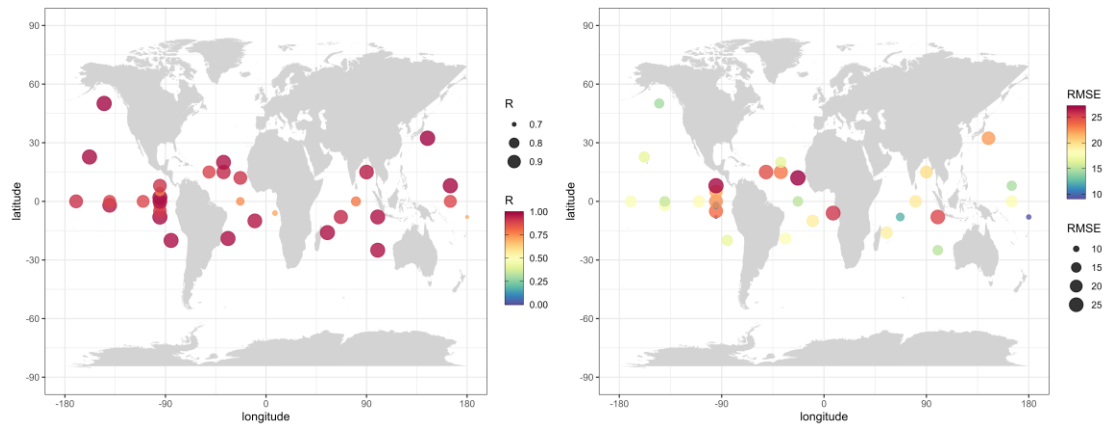


**Figure S7.** Spatial distribution of Pearson coefficient R (left panel) and RMSE value (right panel) in the comparison of heat storage derived from J-OFURO3 dataset with buoy observations from 129 stations.

**Fig. S8**
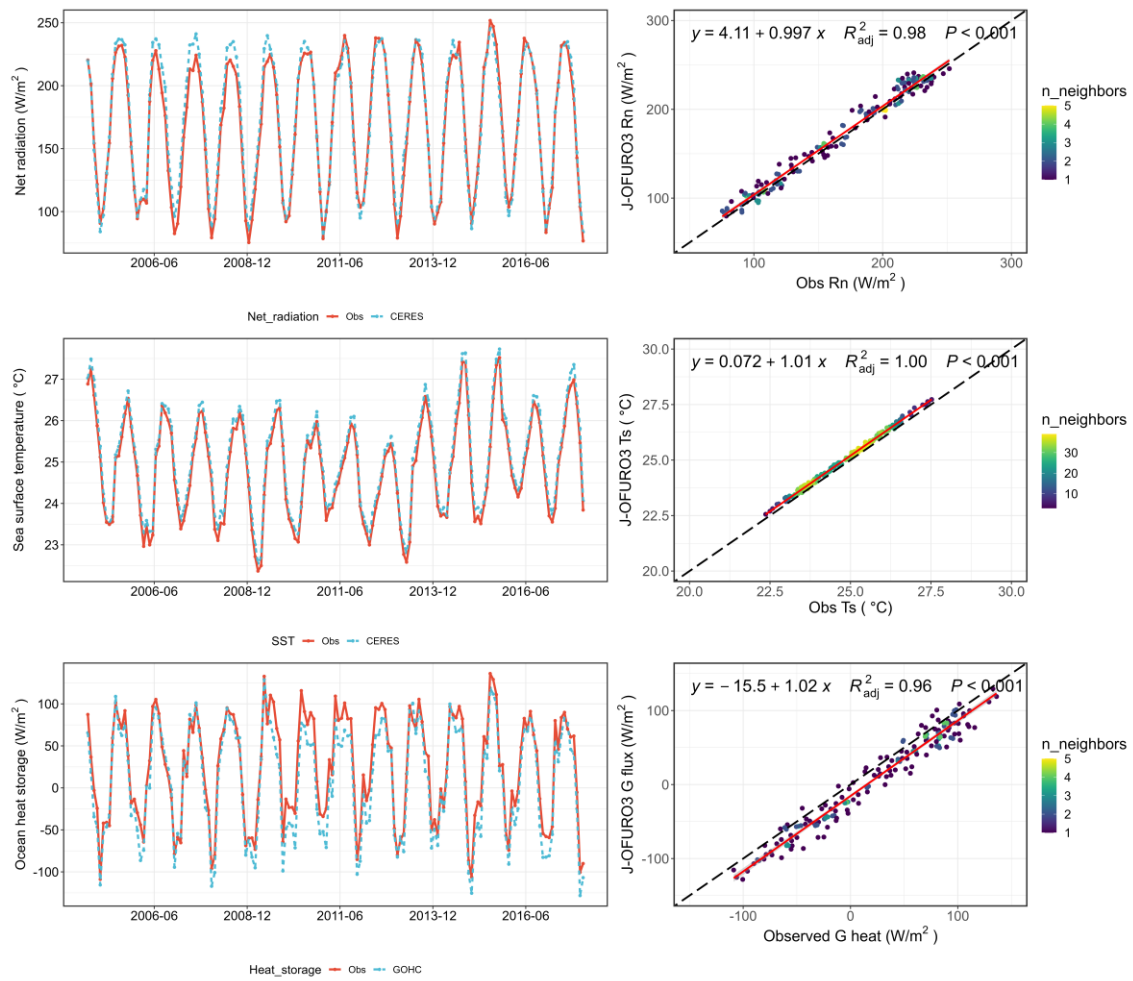


**Figure S8.** Comparisons of time series between estimates extracted from gridded remote sensed datasets and buoy observations: (a) Net radiation, (b) Sea surface temperature, and (c) heat storage at WHOTS station from August 2004 to December 2017.

**Fig. S9**
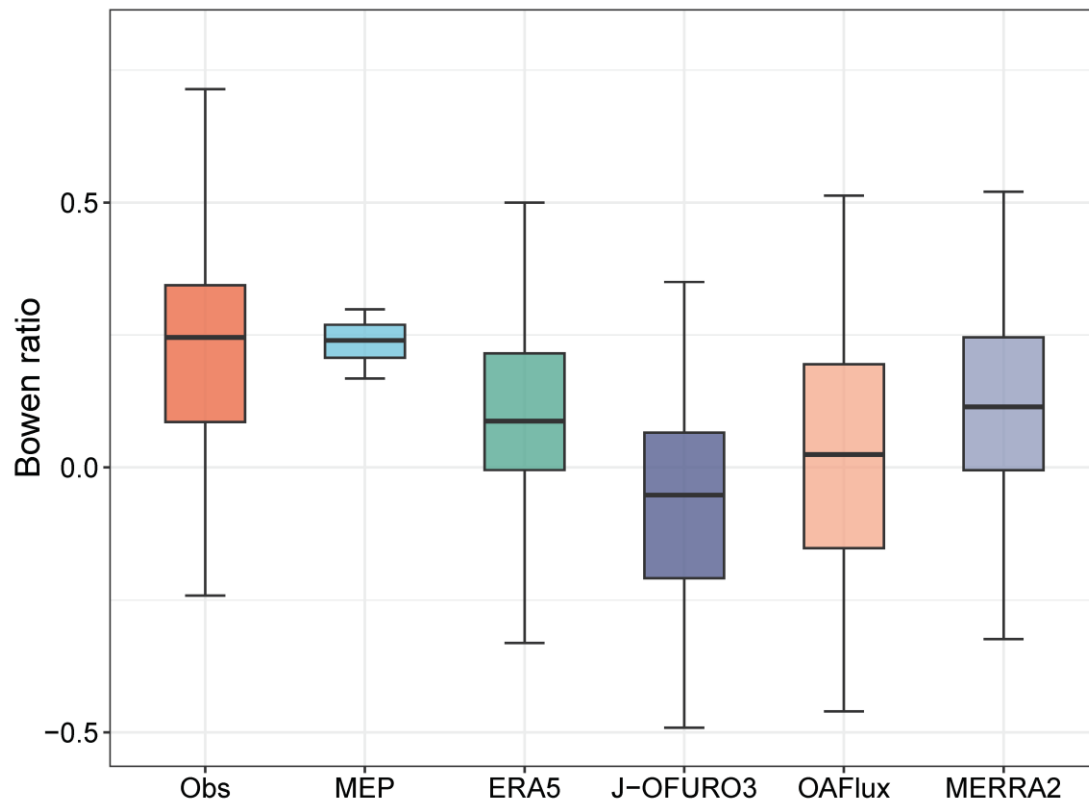


**Figure S9.** Comparison of Bowen ratios extracted from five different gridded products against observations at the PAPA site (144.9°W, 50.1°N) from June 2007 to November 2023. The median values of the Bowen ratio are as follows: Observed (0.23), MEP (0.24), ERA5 (0.07), J-OFURO3 (-0.09), OAFlux (0.01), MERRA2 (0.11).

# Fig. S10
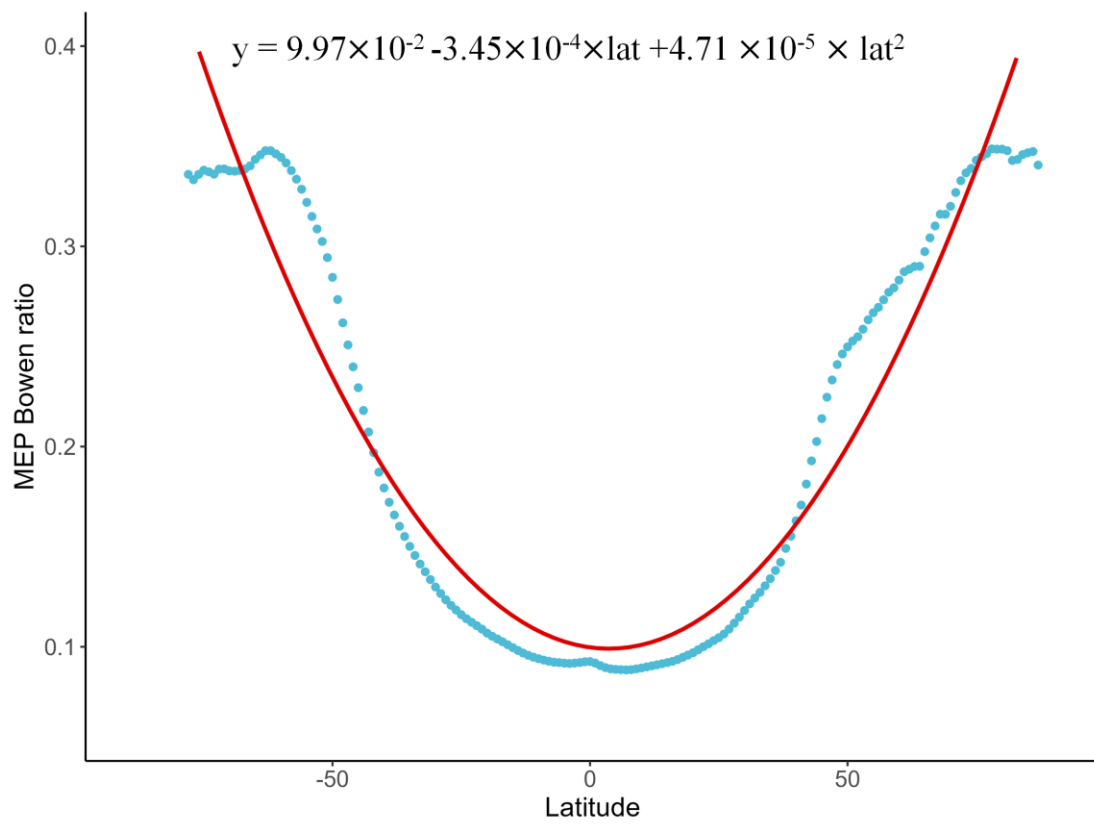


**Figure S10.** A fitted empirical relationship between actual Bowen ratio estimated by the improved MEP model and latitude using a polynomial regression method.

# Table S1.

**Table S1.** The comparisons between changes in ocean heat content ($\Delta$OHC) and observed heat storage ($R_n$-$LE$-$H$) at various ocean depths at the WHOTS buoy site

| Depths of $\Delta$OHC | Linear regression Y=observed $G$, x=$\Delta$OHC | $R^2$ | RMSE (W/m$^2$) |
|---|---|---|---|
| 0~100m | Y=0.92x+22.5 | 0.82 | 34.94 |
| 0~300m | Y=0.61x+22.6 | 0.44 | 57.71 |
| 0~700m | Y=0.41x+23.1 | 0.29 | 74.08 |
| 0~1500m | Y=0.40x+23.0 | 0.32 | 76.07 |
| 0~2000m | Y=0.40x+23.0 | 0.32 | 76.83 |
| 0~3000m | Y=0.40x+23.0 | 0.33 | 77.11 |
| 0~4000m | Y=0.40x+23.0 | 0.33 | 77.08 |
| 0~5000m | Y=0.40x+23.0 | 0.33 | 77.02 |
| 0~6000m | Y=0.40x+23.0 | 0.33 | 77.02 |